

Supplemental Information

**Concerted evolution reveals co-adapted amino acid
substitutions in Na⁺K⁺-ATPase of frogs that prey on toxic toads**

Shabnam Mohammadi, Lu Yang, Arbel Harpak, Santiago Herrera-Álvarez, María del Pilar Rodriguez-Ordoñez, Julie Peng, Karen Zhang, Jay F. Storz, Susanne Dobler, Andrew J. Crawford, and Peter Andolfatto

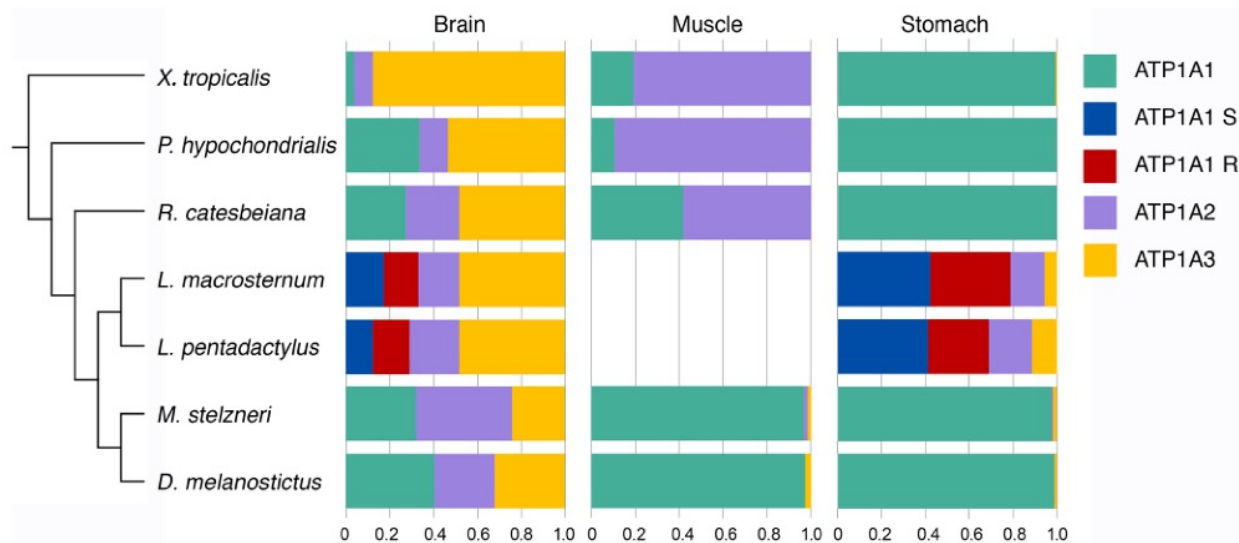


Figure S1. Proportion of ATP1A1, ATP1A2, and ATP1A3 paralogs in brain, muscle, and stomach of seven anuran species, related to Figure 1. RNA-seq reads for eight species were mapped to species-specific copies of ATP1A1, ATP1A2, and ATP1A3 using bwa (see Star Methods). Uniquely mapped reads were counted for each paralog and estimated as a proportion of the sum of the reads for all three ATP1A paralogs. *X. tropicalis*: *Xenopus tropicalis*; *P. hypochondrialis*: *Phyllomedusa hypochondrialis*; *R. catesbeiana*: *Rana catesbeiana*; *L. macrosternum*: *Leptodactylus macrosternum*; *L. pentadactylus*: *Leptodactylus pentadactylus*; *M. stelzneri*: *Melanophryniscus stelzneri*; *D. melanostictus*: *Duttaphrynus melanostictus*.

Family	Species	ATP1A1	ATP1A2	ATP1A3
Human	<i>Homo sapiens</i>	1 1 1 1 1 1 1 1 1 1 1 0 1 1 1 1 1 1 1 1 2 2 8 1 2 4 5 6 7 9 0 2 Y Q A T E E E Q N N	1 1 1 1 1 1 1 1 1 1 1 0 1 1 1 1 1 1 1 1 2 2 8 1 2 4 5 6 7 9 0 2 Y Q A M E D E Q N N	1 1 1 1 1 1 1 1 1 1 1 0 1 1 1 1 1 1 1 1 2 2 8 1 2 4 5 6 7 9 0 2 Y Q A T E D D S G N
Brown rat	<i>Rattus norvegicus</i>	· R S · · · P · D	· L · · · S ·	· · · · · A ·
Lizard	<i>Ameiva ameive</i>	· · · · · N ·	· · · · ·	· · · · ·
Bombinatoridae	<i>Bombina maxima</i>	· · · · D ·	· · · ·	· · · ·
Pipidae	<i>Xenopus tropicalis</i>	· T · · · T ·	· · I · · · I ·	· L · M · E E ·
Pelobatidae	<i>Pelobates fuscus</i>	· · · ·	· · I · · · I ·	· · · · · A ·
Megophryidae	<i>Oreolalax rhodostigmatus</i>	· · · ·	· · I · · · I ·	· · · ·
Megophryidae	<i>Leptobrachium boringii</i>	· · · ·	· · I · · · I ·	· · · · · A ·
Microhylidae	<i>Kaloula pulchra</i>	· · · · D ·	· · I · · · I ·	· · I M · · E I N ·
Mantellidae	<i>Mantella betsileo</i>	· · · ·	· · I · · · I ·	· · M · · A N ·
Dicromystidae	<i>Quasipa boulengeri</i>	· · · · D ·	· · I · · · I ·	· · L · · · N ·
Dicromystidae	<i>Fejervarya cancrivora</i>	· · · · D ·	· · I · · · I ·	· · L · · · N ·
Ranidae	<i>Peleophlyax lessonae</i>	· · · ·	· · I · · · I ·	· · · · · A N ·
Ranidae	<i>Odorrana tormota</i>	· · · ·	· · I · · · I ·	· · M · · A N ·
Ranidae	<i>Rana sphenocephala</i>	· · I M · D · I ·	· · I · · · I ·	· · L · · · N ·
Ranidae	<i>Rana catesbeiana</i>	· · · ·	· · I · · · I ·	· · · · · N ·
Myobatrachidae	<i>Limnodynastes peronii</i>	· · · ·	· · I · · · I ·	· · · · · A N ·
Hylidae	<i>Cyclorana alboguttata</i>	· · · ·	· · I · · · I ·	· · · · · A ·
Hylidae	<i>Phyllomedusa hypochondrialis</i>	· · · ·	· · I · · · I ·	· · · · · A ·
Craugastoridae	<i>Craugastor fitzingeri</i>	· · · ·	· · I · · · I ·	· · · · · A ·
Strabomantidae	<i>Orebates cruralis</i>	· · · ·	· · I · · · I ·	· · · · · A ·
Leptodactylidae	<i>Engystomops pustulosus</i>	· · · ·	· · I · · · I ·	· · · · · A ·
Leptodactylidae	<i>Lithodytes lineatus</i>	· · · · D ·	· · I · · · I ·	· · · · · A ·
Leptodactylidae	<i>Leptodactylus macrosternum</i> S	· · · ·	· · I · · · I ·	· · · · · A ·
Leptodactylidae	<i>Leptodactylus macrosternum</i> R	· R T · · D · · D	· · I · · · I ·	· · · · · T ·
Dendrobatidae	<i>Dendrobates auratus</i>	· · I · · · I ·	· · I · · · I ·	· · · · · N A N ·
Bufonidae	<i>Melanophryniscus stelzneri</i>	H L V · · D · N · ·	· · I · · · M · ·	· · · · · E R ·
Bufonidae	<i>Atelopus zeteki</i>	· R K S D L · D · ·	· T V I · · D T · ·	· R K S D L E D N ·
Bufonidae	<i>Duttaphrynus melanostictus</i>	· R K S D L · D · ·	· T V I · · D T · ·	· L · · · E · R ·
Bufonidae	<i>Bufoates viridis</i>	· R K S D L · D · ·	· R K S D L E D N ·	· L · · · E · R ·
Bufonidae	<i>Rhinella marina</i>	· R K S D L · D · ·	· R K S D L E D N ·	· L · · · E · R ·

Figure S2. Variation among sites implicated in CG-resistance for ATP1A paralogs of various species, related to Figure 1 and 2. Sequences of ATP1A2 and ATP1A3 were reconstructed using the same method as ATP1A1 described in Materials and Methods. Consensus sequences of anuran species were generated in MEGA 7.0 and used as reference for each paralog. Only sites implicated in CG-resistance are shown. Following convention, positions of substitutions, shown at the top, are aligned relative to the sheep (*Ovis aries*) sequence NM_001009360 subtracting 5 AA from 5'end (e.g., the first position is 108). A dot indicates identity with the reference sequence. ATP1A1S and ATP1A1R of *Leptodactylus macrosternum* are indicated in blue and red, respectively. Bufonid (toad) species, the prey species that produce CG toxins, are highlighted in purple. Blank: missing data. We failed to identify an ortholog of ATP1A4 in any of the available anuran genome assemblies, including our assembly of *Leptodactylus fuscus*.

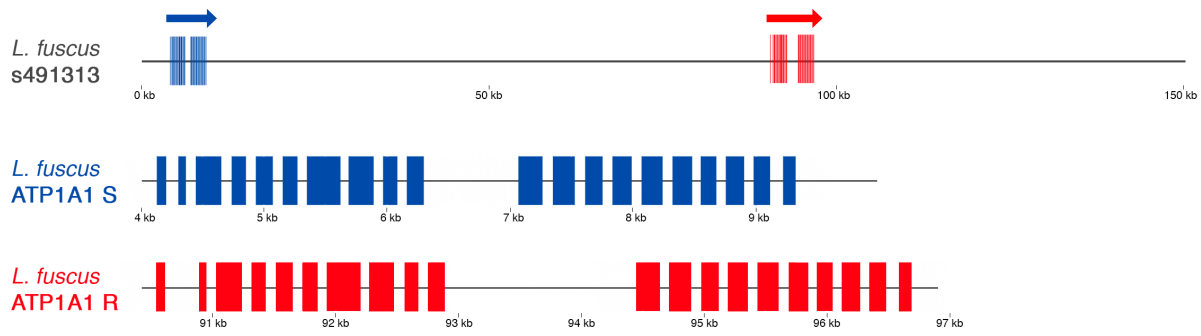


Figure S3. Annotation of ATP1A1S and ATP1A1R paralogs in the *Leptodactylus fuscus de novo* genome assembly, related to Figure 3. ATP1A1S (blue) and ATP1A1R (red) occur in tandem on scaffold s491313 (Genbank Acc# MT422194 and MT422195) ~80 kilobases apart. The boundary between exons and introns was determined by BLAST and manual correction (*i.e.*, ensuring that each intron started with GT and ended with AG). The gene structure figures were plotted with ggbio in R.

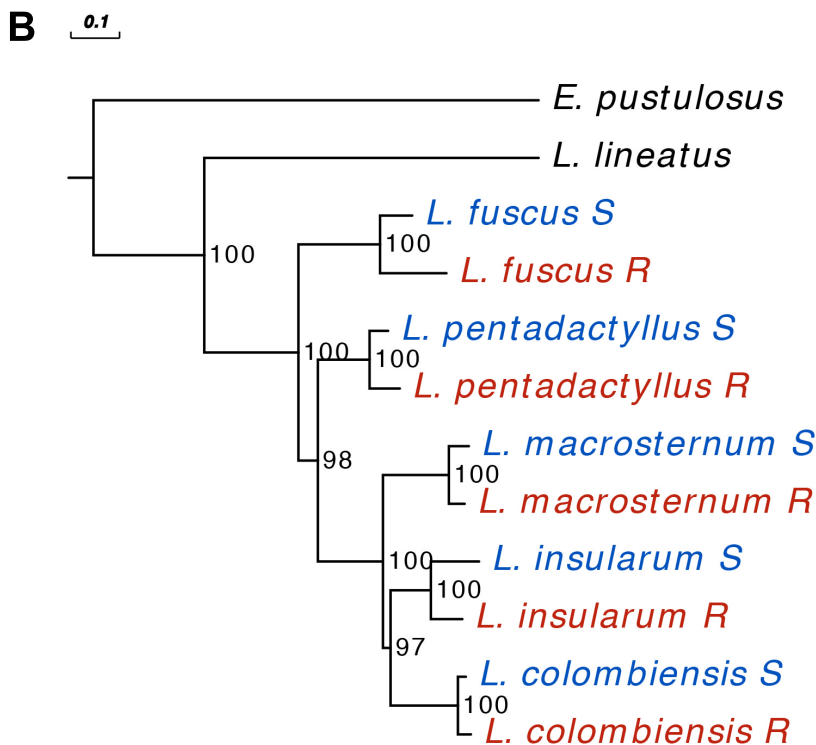
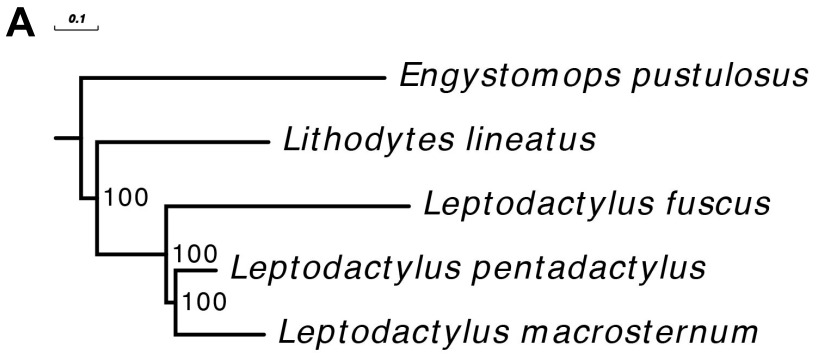


Figure S4. **A)** A species tree of *Leptodactylus* and outgroup species, related to Figure 1. The phylogenetic tree was constructed using an alignment of 813 orthologous mRNA sequences under the best partition model with IQ-TREE 2.0.4 (see Star Methods). Branch lengths: (*Engystomops pustulosus*:0.699436, (*Lithodytes lineatus*):0.395135, (*Leptodactylus fuscus*):0.559378, (*Leptodactylus pentadactylus*): 0.092965, *Leptodactylus macrosternum*: 0.203845)100:0.0216082)100:0.159296)100:0.0368124). **B)** A phylogenetic tree of ATP1A1 based on intron sequences, method same as above.

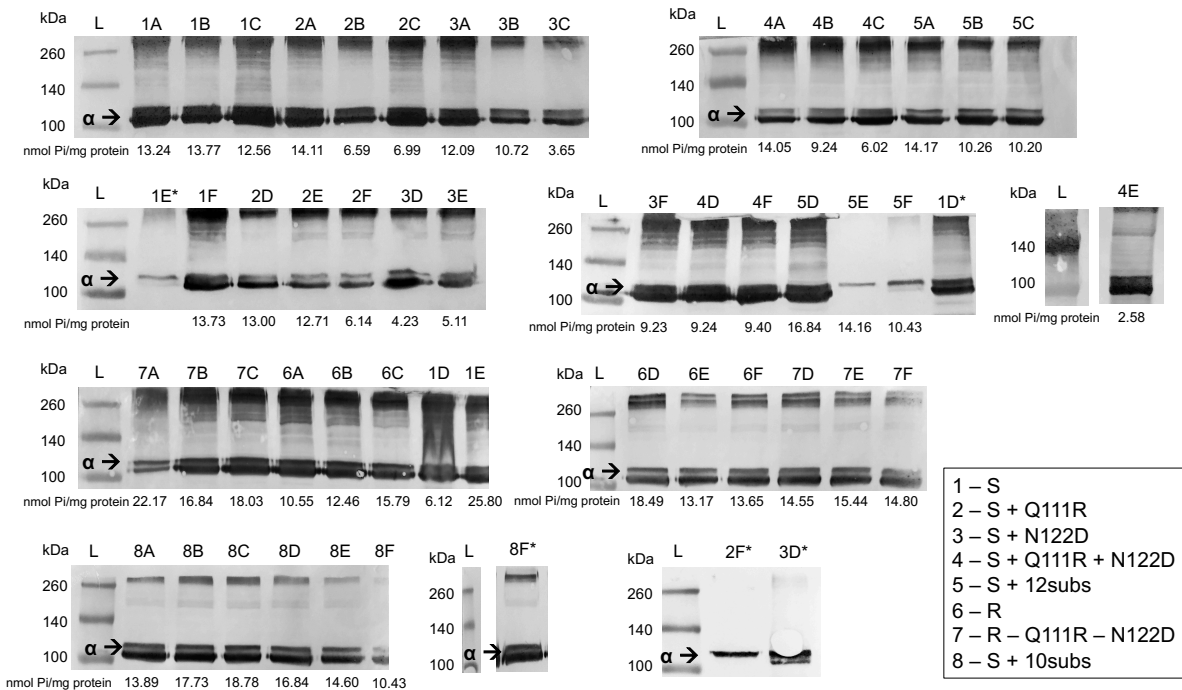


Figure S5. Western blot analysis of Na^+,K^+ -ATPase with engineered ATP1A1 (α) subunits produced in this study, related to Figure 5. The western blots confirm the expression of recombinant Na^+,K^+ -ATPase through cell culture. The 110 kDa ATP1A1 protein is stained with the $\alpha 5$ monoclonal antibody followed by a horseradish peroxidase conjugated goat antimouse antibody. Samples represent six biological replicates of eight different recombinant Na^+,K^+ -ATPase (Table S5). The protein ladder is indicated by an “L” above it. Each panel represents one gel. In two cases (4E and 8F*) sample were run on separate gels thus only the ladder and single sample lane are shown. Samples that were run a second time due to poor western blot quality are indicated by an asterisk (original runs are also included in this figure). ATPase activity levels (nmol $\text{Pi}/\text{mg protein}$) of each biological replicate are indicated under its respective band. ATPase activity is omitted for the repeated runs (indicated by asterisk).

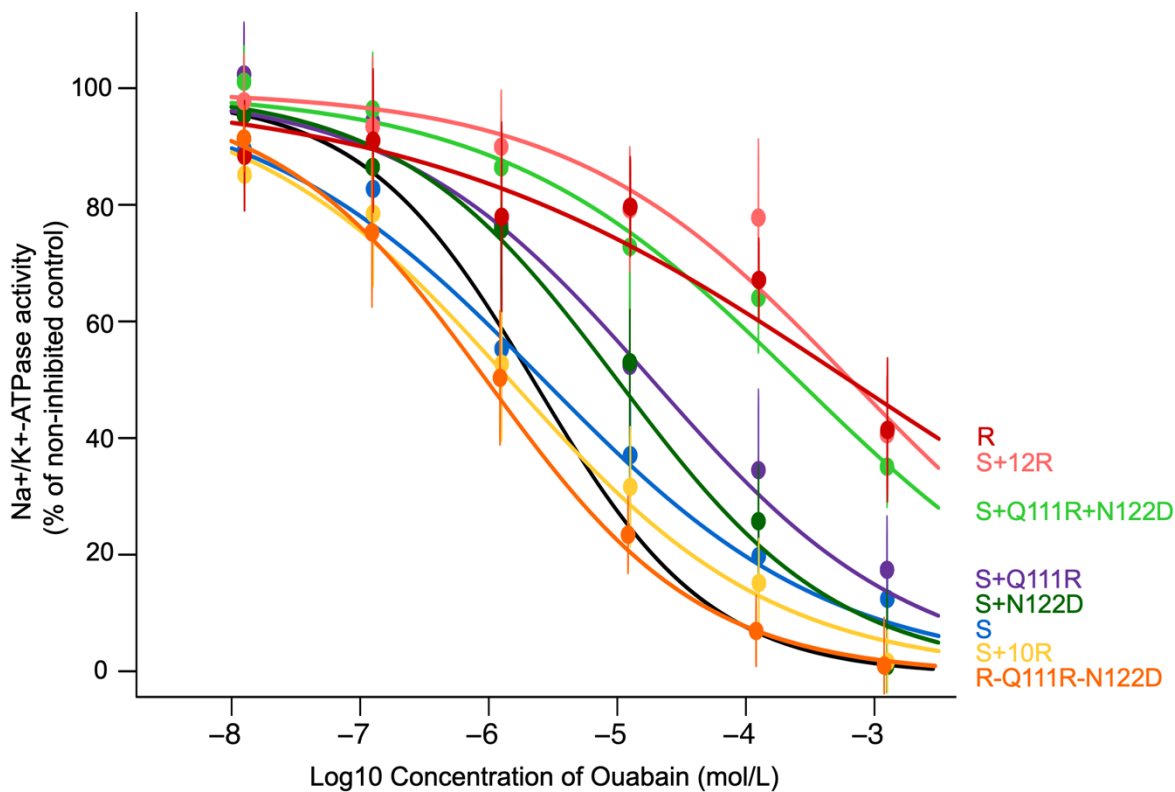


Figure S6. Cardiotonic steroid (ouabain) inhibition curves for six each engineered *Leptodactylus* Na^+,K^+ -ATPase produced in this study, related to Figure 5. Points and error bars represent the mean \pm SEM ($n=6$ biological replicates) percentage of protein activity relative to controls measured in the absence of ouabain and excluding the activity of background ATPases. The black inhibition curve was measured from commercially procured porcine cerebral cortex (CAS 9000-83-3, Sigma-Aldrich, Inc.) and represents a standard benchmark reference for cardiotonic steroid sensitivity ($\text{Log10 } \text{IC}_{50} = -5.61$). The ATP1B1 of *Leptodactylus macrosternum* was co-expressed with each engineered version of ATP1A1 (Table S5).

Species	Museum ID	Field ID	Data type	Locality	Latitude, longitude
<i>Engystomops pustulosus</i>		AJC 3734	RNA-seq	Mariquita, Tolima, CO.	05.2635, -074.891
<i>Engystomops pustulosus</i>		JSM 228	intron	Zambrano, Bolívar, CO	09.75, -074.8333
<i>Lithodytes lineatus</i>		AJC 6408	RNA-seq	El Cachivero, Meta, CO.	
<i>Lithodytes lineatus</i>	ANDES-A 2536	AJC 2406	intron	Trubon, Río Vaupés, Vaupés, CO.	01.21, -070.62
<i>Leptodactylus fuscus</i>	ANDES-A 3141	AJC 5344	plasmid	Neiva, Huila, CO.	02.8796, -075.2757
<i>Leptodactylus fuscus</i>		JSM 205	genome	Garzón, Huila, CO.	02.2058, -075.6440
<i>Leptodactylus pentadactylus</i>	ANDES-A 2327	AJC 4761	RNA-seq	Leticia, Amazonas, CO.	-03.865, -070.2061
<i>Leptodactylus pentadactylus</i>	ANDES-A 949	JMP 2179	intron	Leticia, Amazonas, CO.	-04.10592, -069.25
<i>Leptodactylus macrosternum</i>		AJC 3653	RNA-seq	Puerto Carreño, Vichada, CO.	06.10, -067.483
<i>Leptodactylus macrosternum</i>	ANDES-A 1148	AJC 3430	intron	Orocué, Casanare, CO.	04.9093, -071.4286
<i>Leptodactylus insularum</i>	ANDES-A 3146	AJC 5345		Neiva, Huila, CO.	02.8441, -075.3328
<i>Leptodactylus insularum</i>		AJC 3752	CDS	Montería, Córdoba, CO.	08.7917, -075.8629
<i>Leptodactylus insularum</i>		JSM 261	intron	Barú, Bolívar, CO.	10.1458, -075.6792
<i>Leptodactylus colombiensis</i>		AJC 5510		Santa María, Boyacá, CO.	04.8499, -073.2653
<i>Leptodactylus colombiensis</i>	ANDES-A 3066	AJC 3755	CDS	Nilo, Cundinamarca, CO.	04.3584, -074.5649
<i>Leptodactylus colombiensis</i>		AJC 4301	intron	San Martín, Meta, CO.	03.6969, -073.6986

Table S1. Collection information for samples of leptodactylid frogs used in this study, related to Figure 1. ANDES-A refers to the Amphibian collection of the *Museo de Historia Natural C. J. Marinkelle* of the Universidad de los Andes, Bogotá, Colombia. Collector acronyms are Andrew J. Crawford (AJC), Juan Salvador Mendoza (JSM), Juan Manuel Padial (JMP). All collecting sites are located in Colombia (CO). Samples without museum voucher IDs are in the process of being accessioned into the ANDES-A collection.

Species	Data type and format	GenBank Accession
<i>Atelopus zeteki</i>	RNA-seq, PE 140 bp	skin: SRR11583991
<i>Bombina maxima</i>	RNA-seq, PE 90 bp	skin: SRR566619
<i>Bufo viridis</i>	RNA-seq, PE 100 bp	SRR2163277
<i>Craugastor fitzingeri</i>	RNA-seq, SE 100 bp	skin: SRR1560905
<i>Cyclorana alboguttata</i>	RNA-seq, SE 105 bp	muscle: SRR619475
<i>Dendrobates auratus</i>	RNA-seq, PE 150 bp	brain: SRR11583990 muscle: SRR11583979 stomach: SRR11583968 CDS: MT813444
	<i>de novo</i> assembly	
<i>Duttaphrynus melanostictus</i>	RNA-seq, PE 150 bp	brain: SRR11583966 muscle: SRR11583965 stomach: SRR11583964 CDS: MT813445
	<i>de novo</i> assembly	
<i>Engystomops pustulosus</i>	RNA-seq, PE 140 bp	brain: SRR11583963 stomach: SRR11583962 CDS: MT396181 partial gene: MT422192
	<i>de novo</i> assembly	
	long-read sequencing	
<i>Fejervarya cancrivora</i>	RNA-seq, PE 100 bp	SRR1554290
<i>Homo sapiens</i>	NCBI reference sequence	NM_001160233.1
<i>Kaloula pulchra</i>	RNA-seq, PE 150 bp	muscle: SRR11583961 stomach: SRR11583989 CDS: MT813446
	<i>de novo</i> assembly	
<i>Leptobrachium boringii</i>	RNA-seq, PE 100 bp	SRR4436787
<i>Leptodactylus colombiensis</i>	cloning, plasmid sequencing	CDS: MT396187 (ATP1A1S) MT396188 (ATP1A1R)
	long-read sequencing	partial gene: MT422198 (ATP1A1S) MT422199 (ATP1A1R)
<i>Leptodactylus fuscus</i>	cloning, plasmid sequencing	CDS: MT396183 (ATP1A1S) MT396184 (ATP1A1R)
	single-molecule genomic sequencing	<i>de novo</i> assembly: GitHub: https://github.com/AndolfattoLab/Leptodactylus-fuscus-genome partial gene: MT422194 (ATP1A1S) MT422195 (ATP1A1R)
<i>Leptodactylus insularum</i>	cloning, plasmid sequencing	CDS: MT396191 (ATP1A1S) MT396192 (ATP1A1R)
	long-read sequencing	partial gene: MT422202 (ATP1A1S) MT422203 (ATP1A1R)
<i>Leptodactylus macrosternum</i>	RNA-seq, SE 140 bp	brain: SRR11583988 stomach: SRR11583987
	<i>de novo</i> assembly	CDS: MT396189 (ATP1A1S) MT396190 (ATP1A1R)
	long-read sequencing	partial gene: MT422200 (ATP1A1S) MT422201 (ATP1A1R)
<i>Leptodactylus pentadactylus</i>	RNA-seq, SE 140 bp	brain: SRR11583986 stomach: SRR11583985
	<i>de novo</i> assembly	CDS: MT396185 (ATP1A1S)

		MT396186 (ATP1A1R)
	long-read sequencing	partial gene: MT422196 (ATP1A1S) MT422197 (ATP1A1R)
<i>Limnodynastes peronii</i>	RNA-seq, PE 100 bp	SRR8712702
<i>Lithodytes lineatus</i>	RNA-seq, PE 75 bp <i>de novo</i> assembly long-read sequencing	muscle: SRR11583984 stomach: SRR11583983 CDS: MT396182 partial gene: MT422193
<i>Mantella betsileo</i>	RNA-seq, PE 90 bp	skin: SRR7592160
<i>Megophrys nasuta</i>	RNA-seq, PE 150 bp <i>de novo</i> assembly	brain: SRR11583982 muscle: SRR11583981 stomach: SRR11583980 CDS: MT813448
<i>Melanophrynniscus stelzneri</i>	RNA-seq, PE 150 bp <i>de novo</i> assembly	brain: SRR11583978 muscle: SRR11583977 stomach: SRR11583976 CDS: MT813449
<i>Odorrana tormota</i>	RNA-seq, PE 150 bp	skin: SRR6896138
<i>Oreobates cruralis</i>	RNA-seq, PE 126 bp	intestine: SRR5507183
<i>Oreolalax rhodostigmatus</i>	RNA-seq, PE 150 bp	SRR6265740
<i>Pelobates fuscus</i>	RNA-seq, PE 90 bp	SRR5119616
<i>Pelophylax lessonae</i>	RNA-seq, PE 90 bp, PE	SRR1164893
<i>Quasipaa boulengeri</i>	RNA-seq, PE 100 bp, PE	SRR2962603
<i>Rana catesbeiana</i>	RNA-seq, PE 150 bp <i>de novo</i> assembly	brain: SRR11583975 muscle: SRR11583974 stomach: SRR11583973 CDS: MT813450
<i>Rana sphenocephala</i>	RNA-seq, PE 150 bp <i>de novo</i> assembly	brain: SRR11583972 muscle: SRR11583971 stomach: SRR11583970 CDS: MT813451
<i>Rattus norvegicus</i>	NCBI reference sequence	NM_012504.1
<i>Rhinella marina</i>	RNA-seq, PE 140 bp <i>de novo</i> assembly	brain: SRR11583969 skin: SRR11583967 CDS: MT813452
<i>Xenopus tropicalis</i>	NCBI reference sequence	NM_204076.1

Table S2. Sources of ATP1A1 sequences included in the phylogenetic analysis, related to Figure 1. New data generated by this study are indicated by blue text (RNA-seq datasets: GenBank PRJNA627222, genome assembly: GitHub <https://github.com/AndolfattoLab/Leptodactylus-fuscus-genome>).

Sequencer	HiSeq X
Assembly software	Supernova 2.1.1
Number of reads	775.95 million
Read format	Paired-end 150 nt
Effective read depth coverage	48.35
Estimated genome size	2.42 Gb
Weighted mean molecule size	29.36 kb
Number of scaffolds >= 10 kb (long scaffolds)	16,530
N50 contig size	19.69 kb
N50 scaffold size	362.61 kb
Assembly size (only scaffolds >= 10 kb)	1.26 Gb
<hr/>	
BUSCO version	4.0.5
Lineage dataset	Tetrapoda_odb10
Input genome format	Supernova_pseudohap2_2
Total groups searched	5310
Complete BUSCOs	3182 (60.0%)
Complete and single-copy BUSCOs	3041 (57.3%)
Complete and duplicated BUSCOs	141 (2.7%)
Fragmented BUSCOs	669 (12.6%)
Missing BUSCOs	1459 (27.4%)

Table S3. Summary of the *de novo* genome assembly of *Leptodactylus fuscus*, related to Figure 1.

Construct Name	Engineered Substitution(s)	Description	Ouabain sensitivity (mol/L) Mean(log ₁₀ IC ₅₀) ± SD	ATPase activity nmol Pi/(mg protein*min) ± SD
S	-	Sensitive (S) paralog of <i>L. macrosternum</i> ATP1A1	-5.63 ± 0.59	16.30 ± 5.01
S+Q111R	Q111R	Q111R on the S paralog background	-4.89 ± 0.85	10.68 ± 3.71
S+N122D	N122D	N122D on the S paralog background	-5.06 ± 0.66	7.16 ± 3.62
S+Q111R+N122D	Q111R + N122D	Q111R and N122D on the S paralog background	-3.62 ± 0.28	8.29 ± 3.86
S+10subs	A112T, E116D, I135V, L180Q, I199L, I279V, S403C, L536M, Q701L, I788M	All substitutions strongly distinguishing R and S paralogs, except Q111R and N122D, on the S paralog background	-5.82 ± 0.47	16.37 ± 3.05
R-Q111R-N122D	R111Q, D122N	Reversions R111Q and D122N on the R paralog background	-5.60 ± 0.33	17.41 ± 2.87
S+12subs	Q111R, A112T, E116D, N122D, I135V, L180Q, I199L, I279V, S403C, L536M, Q701L, I788M	Twelve substitutions strongly distinguishing R and S paralogs on the S paralog background	-3.23 ± 0.75	12.17 ± 2.43
R	-	Resistant (R) paralog of <i>L. macrosternum</i> ATP1A1	-3.25 ± 0.77	14.09 ± 2.77

Table S4. List of engineered ATP1A1 constructs used to test functional effects of amino acid substitutions in *Leptodactylus* including summary of the ouabain sensitivity and catalytic properties of Na⁺,K⁺-ATPase for each ATP1A1 construct, related to Figure 5. The values represent the mean and standard deviation (SD) ouabain sensitivity (log₁₀IC₅₀) of ATPase activity of six biological replicates. ATP1B1 of *Leptodactylus macrosternum* was co-expressed with ATP1A1.

Note: R and S paralogs of *L. macrosternum* differ by the 12 substitutions that are the focus of this study and by 9 additional amino-acid substitutions and a two-amino acid insertion-deletion difference. Our experiments revealed that these 10 *L. macrosternum*-specific substitutions do not contribute detectably to S vs. R differences in CG resistance of enzyme function (using all 10 as one co-variate, ANOVA p>0.5. Following convention, positions of substitutions are standardized relative to the sheep (*Ovis aries*) sequence NM_001009360 - 5 AA from 5' end.

(Explanatory Variables) ANOVA	Ouabain sensitivity $\log_{10}(\text{IC}_{50})$				ATPase activity nmol Pi/(mg protein*min)			
	df	MS	F	p value	df	MS	F	p value
Q111R	1, 42	42.8	107. 8	2.7e-13	1, 42	83.0	6.9	0.015
N122D	1, 42	11.8	27.7 2	2.3e-6	1, 42	101.4	7.98	7.2e-3
10subs	1, 42	0.59	1.6	0.22	1, 42	228.1	17.96	1.2e-4
R-S background	1, 42	0.04	1.9	0.74	1, 42	11.5	0.34	0.34
Q111R:N122D	-	-	-	-	1, 42	7.6	5.64	0.022

(Explanatory Variables) Linear regression	Ouabain sensitivity $\log_{10}(\text{IC}_{50})$				ATPase activity nmol Pi/(mg protein*min)			
	Est	SE	t	p value	Est	SE	t	p value
Intercept	-6.03	0.17	-36.3	<2e-16	14.3	1.19	12.1	3e-15
Q111R	1.32	0.21	6.27	2.7e-13	-4.39	1.88	-2.34	0.024
N122D	1.14	0.21	5.45	2.3e-6	-6.81	1.88	-3.63	7.7e-4
10subs	0.26	0.22	1.19	0.24	1.94	1.46	17.96	0.18
R-S background	-0.08	0.26	-0.34	0.74	1.39	1.46	0.34	0.35
Q111R:N122D	-	-	-	-	6.90	2.91	5.64	0.022

Table S5. Statistical analysis of ouabain sensitivity and ATPase activity, related to Figure 5.
Significant p values are highlighted in bold.

Note: “R-S background” in the ANOVA refers to 9 additional amino acid substitutions and a two amino acid insertion-deletion difference that distinguishes the R and S constructs (derived from *Leptodactylus macrosternum*).

Species	Primer
<i>Engystomops pustulosus</i>	N-terminal Forward: EP_wwBC6_1F GATGTAGAGGGTACGGTTGAGGCACATGGCGGCAAGAAGAA Reverse: EP_wwBC6_11R GATGTAGAGGGTACGGTTGAGGCACATGGCGGCAAGAAGAA C-terminal Forward: EP_wwBC7_11F GGCTCCATAGGAACTCACGCTACTGATCCTGGACCGATGCTCCA Reverse: EP_wwBC7_19R GGCTCCATAGGAACTCACGCTACTGACAATGCTGACGAAGAAGGC
<i>Lithodytes lineatus</i>	Forward: Lep_wwBC3_1F TACATGCTCTGTTAGGGAGGACATGGCGGCAAGAAGAA Reverse: Lep_wwBC3_21R TACATGCTCTGTTAGGGAGGAGGCACAGAACCAACCATGT
<i>Leptodactylus pentadactylus</i>	Forward: Lep_wwBC5_1F ACAGCATCAATGTTGGCTAGTTGACATGGCGGCAAGAAGAA Reverse: Lep_wwBC5_21R ACAGCATCAATGTTGGCTAGTTGAGGCACAGAACCAACCATGT
<i>Leptodactylus macrosternum</i>	Forward: Lep_wwBC2_1F AGGTGATCCAACAAGCGTAAGTAACATGGCGGCAAGAAGAA Reverse: Lep_wwBC2_21R AGGTGATCCAACAAGCGTAAGTAAGGCACAGAACCAACCATGT
<i>Leptodactylus insularum</i>	Forward: Lep_wwBC1_1F AACGGAGGAGTTAGTGGATGATCACAGGCACAGAACCAACCATGT Reverse: Lep_wwBC1_21R AACGGAGGAGTTAGTGGATGATCACAGGCACAGAACCAACCATGT
<i>Leptodactylus colombiensis</i>	Forward: Lep_wwBC8_23F AGAGGGTACTATGTGCCTCAGCACAAGTATGAGCCCGAGCCACTTC Reverse: Lep_wwBC8_3044R AGAGGGTACTATGTGCCTCAGCACCCAGGGCTCGTCTGATGATTAA
<i>Leptodactylus macrosternum</i>	Cloning primer for ATP1B1 amplification from cDNA. Forward: ATCCTCGAGATGGCCAGAGACAAAACCAAGGA Reverse: ATCCTCGAGATGGCCAGAGACAAAACCAAGGA
<i>Leptodactylus macrosternum</i>	Cloning primer for ATP1A1 amplification from cDNA. Forward: TAATACTAGTATGGGATACGGGGCCGGACGTGATGAGTATGAGCCCGAGCCACT Reverse: ACTGCGGCCGCTTAATAATAGGTTCTTCTCCA
<i>Leptodactylus macrosternum</i>	Cloning overhang primer for ATP1A1-R variant amplification from truncated version of gene in TOPO-TA vector. Forward: TAATACTAGTATGGGATACGGGGCCGGACGTGATGAGTATGAGCCCGAGCCACT TCTGAACATGGCGGCAAGAAGAAAGGCAAAGGGAAGGATAAGGAT Reverse: ACTGCGGCCGCTTAATAATAGGTTCTTCTCCA GATTATCAGTTTCGGATTTCATCATATATGAAGATGAGCAGAGAGTAGGGGAAG GCACAGAACCAACCATGTTGGTTCAGTGGGTACATGCGGAGTGCCACATCCATGCC TGGG
<i>Leptodactylus</i> (all species)	Sequencing primer for ATP1A1 from cDNA. Forward: ATAAGTATGAGCCCGAGCC Reverse: CCAGGGCTCGTCTGATTATG

Table S6. List of primers used in this study, related to Figures 1 and 5.